Adaptive Kalman-Based Constrained Predictive Control With Neural Estimator for a Noninverting Buck–Boost Converter

Omid Asvadi-Kermani, *Graduate Student Member, IEEE*, Arman Oshnoei, *Senior Member, IEEE*, and Frede Blaabjerg, *Fellow, IEEE*

***Abstract*—This article introduces an adaptive constrained model predictive control (AMPC) method for regulating the voltage of a noninverting dc buck–boost converter, capable of delivering up to 48 W output. The approach incorporates constraints on the control signal and its variations to minimize oscillations in both input current and output voltage. The AMPC controller employs a linear model, adaptively estimated via an online Kalman-based recursive least squares algorithm. To efficiently manage the computational demands of the AMPC algorithm, a dynamic neural network (DNN), trained using AMPC controller data, is utilized for control within a specific range of the output voltage's steady-state response. A constrained control variable tuning mechanism has been applied to the output of the DNN to reduce the oscillations of the steady-state response more efficiently. Experimental tests have been conducted to assess performance under varying conditions of reference voltage, load, and input voltage. Notably, the fluctuations in output voltage are lower compared to the basic AMPC, another constrained model predictive control, and a PI method. More specifically, for the proposed method, the output voltage fluctuation is about 72%, the calculation time is about 75%, and the minimum energy loss of the switch is about 8.5–10% average less than the basic AMPC.**

***Index Terms*—Adaptive control, dynamic neural networks, model predictive control, noninverting buck–boost converter, steady-state response.**

I. Introduction

DC converters have been extensively utilized in various commercial and industrial systems for adjusting voltage within different ranges [1] and managing output power [2], owing to their advantageous characteristics and efficient performance in recent years. For instance, these converters are employed in the low voltage and current spectrum to regulate the output voltage of solar photovoltaic cells [3]. Given these considerations, it is crucial to focus on maintaining the simplicity and cost-effectiveness of the converter, while enhancing its performance through the implementation of more efficient control strategies. The noninverting buck–boost converter, notable for its effectiveness in both stepping up and stepping down voltage and its straightforward design, has been the primary subject of this study [4]. Its versatility allows for its application in numerous fields, either independently or in conjunction with other converters. Model predictive control is an advanced method of control increasingly employed in recent years across various applications [5], [6], including Microgrids [7], power electronics converters [8], [9], and electrical drives [10] owing to its desirable characteristics such as robust closed-loop stability. Subsequently, an overview of the research focusing on the implementation of this method, highlighting the existing gaps in these studies will be provided. In [11], a dynamic, neural-based, constrained model predictive control (MPC) was implemented on an interleaved boost converter. The deep neural network model utilized possesses a substantial number of parameters, yet lacks an adaptive mechanism for online model parameter estimation. Throughout the control algorithm's execution, the constrained optimization algorithm is executed repeatedly, resulting in a significant computational burden on the control board's CPU. In [12], the unconstrained generalized predictive control was applied to a noninverting buck–boost converter. The model described therein represents the small-signal model of the system's input and output, without directly considering the input current of the converter. The effectiveness of the system's model is crucial, as it significantly influences the controller's performance. This implementation does not impose constraints on the control variable and its variations, leading to unconstrained optimization. This approach could potentially compromise system stability in the event of sudden dynamic changes. Additionally, the output power and voltage tested were notably low. In [13], an unconstrained MPC was implemented on a noninverting buck–boost converter. The article highlights the use of direct MPC (DMPC) to effectively eliminate the dead zone in power electronics converters. DMPC stands out for its ability to handle complex control challenges like plant nonlinearities, multiple inputs, and objectives while ensuring

Received 12 August 2024; revised 16 September 2024; accepted 26 October 2024. Date of publication 29 October 2024; date of current version 18 December 2024. This work was supported in part by the Innovation Fund Denmark under the Project of Artificial Intelligence for Next-Generation Power Electronics (AI-Power), and in part by Independent Research Fund Denmark under Grant 1031-00024B. Recommended for publication by Associate Editor G. Moschopoulos. *(Corresponding author: Omid Asvadi-Kermani.)*

Omid Asvadi-Kermani is with the Faculty of Electrical and Computer Engineering, University of Tabriz, Tabriz 51666-16471, Iran (e-mail: o.asvadikermani@modares.ac.ir).

Arman Oshnoei and Frede Blaabjerg are with the Department of Energy (AAU Energy), Aalborg University, 9220 Aalborg, Denmark (e-mail: aros@energy.aau.dk; fbl@energy.aau.dk).

Color versions of one or more figures in this article are available at https://doi.org/10.1109/TPEL.2024.3487892.

Digital Object Identifier 10.1109/TPEL.2024.3487892

optimal control without the need for a demodulator. This direct control approach uses a more accurate model, which includes switching nonlinearities, resulting in superior performance for some dc converters compared to traditional methods. However, DMPC's major drawback is its high computational demand, though this is somewhat offset by advances in processing speeds and efficient computational techniques. Another DMPC drawback is that the switching pulses are limited to fixed sampling times, which can restrict the minimum width of the pulses. Xiang et al. [14] introduced an output-error-driven incremental MPC (OEDIMPC) for buck converters. Unlike traditional methods, OEDIMPC determines the optimal rate of change for the duty cycle using a reduced-state output-error-driven prediction model. This approach ensures zero steady-state error despite parameter variations, enhances dynamic performance, and requires only one voltage sensor without an observer. The exact model of the system has been used without the online adaptive mechanism. In [15], a robust MPC controller implemented on a float interleaved boost converter, with its proposed control algorithm based on robust model predictive control using convex hull approximation was investigated in [16] the optimization algorithm includes a constraint on the system output, but only steady-state response is specified, and there are no results about inductors currents. Table I summarizes relevant studies related to this topic in the general form.

In [17], a model predictive controller was applied to a noninverting boost converter. The controller utilized the exact nonlinear state-space model, incorporating complex mathematics for stability analysis and design. It is noted that the control signal change, which remained unconstrained, the control signal itself was designated as the argument of the cost function. This can induce oscillations in the control signal. The control signal was calculated using a noniterative closed-form formulation.

The primary focus of this research is to enhance the performance of the proposed AMPC controller during disturbances, while also minimizing computational load.

In order to make the research practical, the noninverting buck-boost dc converter was chosen to check the results of the controllers, it has a relatively simple structure with two switches and two diodes with only one nonlinear state-space model with two state variables that only It can be controlled with a control variable. The challenges in this research are summarized as follows. Due to the nonlinear nature of the system model, there is a challenge in designing an MPC controller for the system and analyzing its stability. Because MPC controllers depend on the accuracy of the model, there is a challenge in achieving optimal controller performance when there are significant changes in system dynamics and in the presence of external disturbances such as large input voltage variations. The fast dynamics of the converter can lead to overshoot in the input current and output voltage, as well as oscillations, which can increase the energy loss in converter components. Another challenge is the high computational load of the MPC method, especially when implementing it in a constrained manner on the control board processor. The main contribution of this article is the online estimation of the system's state-space linear model, including output voltage and input current, using a recursive algorithm based on the Kalman filter. This approach in the predictive controller lessens the controller's reliance on model accuracy and enhances the stability and performance of the closed-loop system, particularly during changes in system dynamics. In this article, an iterative constrained optimization algorithm is employed in the target controller, which enhances the optimization of the cost function. Furthermore, imposing constraints on the control signal and its variations results in a smoother control signal. This leads to reduced fluctuations in the state variables, especially under varying operating conditions of the system. Three experimental tests are conducted: changing the reference output voltage (test1), the load (test2), and both input voltage and load (test3). To lessen the computational burden of the proposed AMPC, an estimated dynamic neural network model, developed from the data of these three controller tests, is utilized as an alternative regulator within a certain range of the output voltage. This substitution is particularly effective in the system's steady-state response, where the dc converter most often operates. In the final, given that a sophisticated controller like constrained adaptive MPC can effectively manage the buck–boost dc converter, it

TABLE I
GENERAL INVESTIGATION OF SOME PREVIOUS WORKS

Ref	Dynamic Complexity of the Controller
[18]	**Dynamic Complexity of the Controller**: The control method simplifies design by integrating modulator and mode detection into one optimization process, enabling smooth transitions between modes and reducing complexity. However, its scalability and response to rapid load changes need further exploration. **Robustness of the Controller in Presence of Disturbances:** The unconstrained MPC is used to handle voltage variations and disturbances, ensuring stable output and protection against overcurrent. Yet, its robustness against big load variations, switches energy losses, and long-term stability under frequent disturbances, are less examined.
[19]	**Dynamic Complexity of the Controller**: Light implementation scheme for ANN-based explicit MPC (LISABE) enhances EMPC with optimized data and ANN structure, simplifying control but its adaptability to various converters and complex goals needs more research. **Robustness of the Controller in Presence of Disturbances:** The scheme demonstrates robust control under disturbances through a predictive strategy and an ANN trained with attention-based tree-search sampling, ensuring stability. A broader analysis of its performance under various disturbances and the long-term effects of such disturbances is needed.
[20]	**Dynamic Complexity of the Controller**: The flying capacitor bidirectional buck-boost converter uses a specific fixed frequency MPC strategy for easy mode switching, but its suitability for larger systems requires more research. **Robustness of the Controller in the Presence of Disturbances:** The control strategy shows robust performance against voltage variations and disturbances, ensuring stable operation of energy storage applications. Yet, a deeper analysis involving real-world disturbances would better demonstrate its practical robustness
[21]	**Dynamic Complexity of the Controller**: The study introduces an MPC algorithm for the versatile buck-boost (VBB) converter that simplifies control with a digital signal controller (DSC), needing further investigation on scalability and transient response. **Robustness of the Controller in the Presence of Disturbances:** The MPC-based strategy is developed to be robust against disturbances, adjusting to input voltage and load changes to maintain stability. However, the analysis lacks depth on specific challenges like partial shading, with room for further study on long-term impacts.
	Proposed AMPC Method : **Dynamic Complexity of the Controller**: The linear state space model of the converter uses only 2 state variables for simplicity. The AMPC controller minimizes calculation volume by reducing the control and prediction horizon. A simplified DNN model replaces AMPC in steady state, cutting average calculation time by 75% and reducing output voltage fluctuations by 72%. **Robustness of the Controller in the Presence of Disturbances:** Adding the KRLS online model estimation to AMPC has enhanced the controller's performance against disturbances in both buck and boost modes. The proposed controller was tested by simultaneously changing the load and input voltage by 100% and 50%, and by changing the load along with the capacitor and inductor values by 100%.

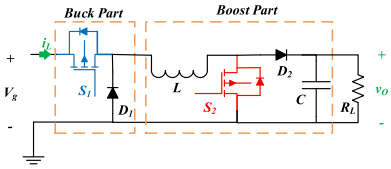

Fig. 1. Circuit diagram of the noninverting buck–boost converter.

TABLE II
DC CONVERTER PARAMETERS, AND EXPERIMENTAL SETUP SPECIFICATIONS

Component	Nominal Value
C	100 μF, 100 V
L	50 μH, $r_{Inductor} = 0.05\ \Omega$
$D_{1,2,}$	MUR1560, 15 A,
$S_{1,2}$	IRFP250 ,$R_{DS} = 0.085\ \Omega$
$R_L\ (load)$	10, 20 Ω
HCPL3120	Mosfet Driver
Current Shunt	0.1 Ω
STM-F446RE,W5500	Control Board, $f_{sw} = 40$ kHz, Ethernet

is expected that approximating this controller using solely a linear dynamic neural network (DNN) when applied to a real system might result in discrepancies from the reference value. These discrepancies are particularly noticeable in steady-state mode due to changes in system conditions. To mitigate this error, a corrective mechanism has been incorporated into the DNN output. This mechanism involves adjusting the duty cycle control variable based on the output voltage error and a constant coefficient, thereby enhancing control precision. Comparative results between the target controller, the basic AMPC, developed MPC in [17] and a PI controller indicate that the target method demonstrates lower fluctuations in output voltage and control variable and lower energy loss in the switches, along with improved adaptive estimation of the model. More specifically, for the proposed method, the output voltage fluctuation is about 72%, the calculation time is about 75%, and the energy loss of the switches is 8.5 to 10% on average less than the basic AMPC. In the end, there is a key point. The AMPC method stands out for its high flexibility. Both constrained AMPC and the DNN model estimation of the controller rely on a data-driven models designed to minimize the number of converter variables. This approach can be applied to various types of dc converters with different complexity.

II. SYSTEM MODEL DESCRIPTION

The schematic of the described noninverting buck–boost converter has been shown in Fig. 1.

According to Fig. 1 and [17], it has been specified in the described converter switch S_1 and diode D_1 are the main components of the buck part and S_2 and diode D_2 are the main components of the boost part of the converter. The specifications of the converter and the experimental setup is specified in Table II. Considering that the main focus of this research was on the efficiency of MPC control methods for buck–boost dc converter, and not on the structure and performance of the converter itself, it is rational to compare this research with related studies. The values of the converter components were chosen according to [17] and existing equipment. Input voltage ranges from 6 to 12 V, output voltage ranges from 6 to 22 V, and maximum output power is 48 W.

A. Bilinear Model of DC–DC Converter

According to [17], the noninverting buck–boost converter can be modeled as a discrete bilinear system. This model is comprised of both a linear and a nonlinear part. All parameters and variables represent real values. $x = [\, i_L, v_O]^T$ is the state vector. i_L is the converter's input current and v_O is the output voltage of the converter. u is the modulation index and the control that has the value in the range of 0–1. T_s is the sampling time and, $T_{sw} = f_{sw}^{-1}$ is the switching time. In this research, to better compare the parameters related to the inductor and capacitor values of the corresponding converter, Garcés-Ruiz et al. [17] has been selected. To verify the selected parameters for the converter, considering the switching frequency of 40 kHz, the equations presented in [22] have been used that show minimum proper value for the converters' parameters for each buck or boost mode that bigger values have been considered as the minimum value in (1c) and, (1d), which will explained as follow. These values have been chosen based on an output power of 48 W, a maximum input voltage (V_g) of 12 V, and output voltages (v_O) of 22 V in boost mode and 6 V in buck mode. The bilinear state-space model is shown in

$$\begin{cases} A = \begin{bmatrix} 1 & \frac{-T_s}{L} \\ \frac{T_s}{C} & 1 - \frac{T_s}{R_L C} \end{bmatrix}, B = \begin{bmatrix} 0 & \frac{T_s}{L} \\ \frac{-T_s}{C} & 0 \end{bmatrix} b = \begin{bmatrix} \frac{T_s V_g}{L} \\ \\ 0 \end{bmatrix} & \text{(1a)} \\ x(k+1) = Ax(k) + Bu(k)\, x(k) + bu(k) & \text{(1b)} \end{cases}$$

$$L_{\min} = \begin{cases} \frac{T_{sw} V_g^2 (v_O - V_g)}{2 P_{out} v_O},\ v_O > V_g\ Degenerate\ to\ Boost \\ \frac{T_{sw} v_O^2 (V_g - v_O)}{2 P_{\text{out}} V_g},\ v_O < V_g\ Degenerate\ to\ Buck \end{cases} \quad \text{(1c)}$$

$$C_{\min} = \begin{cases} \frac{T_{sw} P (v_O - V_g)}{\Delta v_O * v_O^2},\ v_O > V_g\ Degenerate\ to\ Boost \\ \frac{T_{sw}^2 v_O (V_g - v_O)}{8 V_g L \Delta v_O},\ v_O < V_g\ Degenerate\ to\ Buck \end{cases} . \quad \text{(1d)}$$

B. Kalman-Based Recursive Least Squares (KRLS) Model Estimation

According to [23], adaptive control methods are generally classified into two broad categories. The first category includes methods that enhance the controller's adaptive performance by updating the parameters of the model used in the controller's design. The second category consists of methods where the controller's parameters are updated over time, either online, or offline, in response to changes in system conditions. The recursive least squares method (one step ahead method) stands out as a model estimation method. It is advantageous because it can be implemented online, requires a small amount of data,

and offers faster convergence. This method is particularly effective when combined with techniques like the Kalman filter, making it suitable for estimating the model of power electronic systems with rapid dynamics. The nonlinear model (1) has been discussed in the previous section possesses two advantageous features: its discrete nature and the incorporation of two primary state variables, which are controlled by a single signal. However, a significant challenge arises due to the inclusion of a nonlinear component, which complicates the design of controllers and stability analysis, and increases the number of model parameters. This article proposes an innovative approach to address these issues, aiming to enhance the model's adaptability under varying working conditions and to reduce the controller's reliance on precise model accuracy. The solution involves estimating the system's model in real-time through a time-varying linear state space model, as depicted in (2), employing a KRLS algorithm. This method facilitates a quicker convergence of estimated parameters to stable values, unlike conventional approaches that rely on a forgetting factor and experience diminished estimator effectiveness as the covariance of estimated parameter errors decreases. The Kalman filter method, therefore, maintains its dynamic capability for rapid model estimation even after the system stabilizes. This remains effective even in the face of sudden and significant changes in system dynamics, as referenced in [24]. It should be mentioned that the implementation of the MPC on the linear state-space model (2) has less complexity and has easier stability analysis. $a_1, .., a_4$ are elements of the state-space (2) A matrix and b_1 and b_2 are elements of input matrix b

$$A=\begin{bmatrix} a_1(k) & a_2(k) \\ a_3(k) & a_4(k) \end{bmatrix}, B=\begin{bmatrix} 0 & 0 \\ 0 & 0 \end{bmatrix} b=\begin{bmatrix} b_1(k) \\ b_2(k) \end{bmatrix} \tag{2}$$

$$\begin{cases} \theta_{k,\text{new}}=\theta_{k,\text{old}}+K(x-\hat{x}),\ \hat{x}=\psi^T\theta_{k,\text{old}} \\ K=\frac{P_{\text{old}}\psi}{R_2+\psi^T P_{\text{old}}\psi},\ P_{\text{new}}=P_{\text{old}}+R_1-K\psi^T P_{\text{old}} \\ \theta_k=[A|b]^T,\ \psi=[x|u]^T,\ u\rightarrow control\ variable \end{cases} \tag{3}$$

where θ is the parameters matrix, K is the Kalman vector, ψ is the regression vector, and $R_2 * P$ and R_1 are the covariance matrix of the estimated parameters and their changes, respectively, that have specified in (3). R_1 and R_2 are determined by repeating practical three test results that have been described in the introduction section properly.

III. Proposed Combinatorial AMPC Controller

A. Basic Constrained AMPC

MPC is an advanced control technique [23] increasingly utilized in power electronics applications due to its straightforward mathematical framework, robust stability, compatibility with discrete data-driven models, and feasibility for constrained implementations. In this article, constrained MPC is applied to the linear estimated state-space model, as described before, using the KRLS algorithm. The change in the control variable is employed as an argument in the cost function, with an inherent constraint to enhance the smoothness of the control signal and bolster stability. Additionally, a constraint is placed on the control variable to ensure that control output remains within an appropriate range, further aiding stability, as discussed in [25]

$$\begin{cases} H_P, Hc=5\rightarrow \textit{Prediction and Control Horizon} \\ X_P=SS(A,b,x,\Delta u,H_P,Hc)\rightarrow \textit{Prediction Model} \end{cases} \tag{4}$$

$$J=(X_P-Ref)^T W_X (X_P-Ref)+U^T W_u U \rightarrow \text{Cost Function}$$

$$\begin{cases} \Delta u_{\min}\le \Delta u_{\text{MPC}}\le \Delta u_{\max} \\ u_{\min}\le u_{\text{MPC}}\le u_{\max} \end{cases} \rightarrow U(k+1|k+Hc)$$
$$U(k+1|k+Hc)\xrightarrow{\text{Receding Horizon}}\Delta u_{\text{MPC}}(k+1)=U(k+1)$$
$$\Delta u_{\min}=-0.01, \Delta u_{\max}=0.01,\ u_{\min}=0,\ u_{\max}=0.7 \tag{5}$$

$H_P, Hc=5$ are prediction and control horizons. X_P is the vector of the predicted output using the *SS* state-space model (2) in the prediction horizon. Where W_X and W_u are the weighted diagonal matrices of the output and changes in the control variable in the cost function. By increasing the value of W_X, the optimization algorithm will effect more on reducing the steady-state error of the output, and by increasing the value of W_u, The optimization algorithm prioritizes softening the fluctuations in the control signal. This is achieved through the numerical solution of the cost function, which employs the sequential quadratic programming algorithm, limited to a maximum of 50 iterations. The parameters for the weight matrices were determined by conducting repeated experiments and evaluating the outcomes, thereby striking a balance between the two described issues. Furthermore, the parameters relevant to prediction and control horizon, as well as associated constraints, are established similarly. A significant increase in the constraint on the control variable can lead to a substantial overshoot and potentially prevent the output from converging to the reference value. In this study, it can also complicate the comparative estimation process of the model. Reducing this parameter increases the permanent error of the output relative to the reference value. Regarding the restriction applied to the changes in the control variable, if this parameter increases excessively, it will cause fluctuations in the control variable, output voltage, and input current. It can also widen the fluctuation range of the estimated model parameters and decrease the accuracy of the DNN equivalent model of the AMPC controller, thus increasing total energy waste. Given the data-driven nature of this research and the numerical constrained optimization mechanism in the AMPC controller, there is no closed formula for calculating the constraints. These parameters and weight coefficients have been determined through repeated tests to achieve the desired results. In this research, the online sequential quadratic programming algorithm (SQP) is utilized for constrained optimization of the cost function in the controller. The rationale behind selecting this method is outlined below. First, due to its reliance on gradient reduction, the method boasts enhanced speed and accuracy. Second, even though the converter model is estimated online using a linear approach, it fundamentally operates as a nonlinear system. Given that the converter's measured data is employed for model estimation in the target AMPC controller, an optimization algorithm based on gradient reduction, such as online SQP, proves to be a suitable

TABLE III
EXPERIMENTAL TESTS SCENARIOS, $T_s = 1$ MS

Test	V_{ref} (V)	R_L (Ω)	V_g (V)
Basic AMPC for DNN Model Estimation			
Reference	14.5(t=0.65-1.34)	10(t=0.65-1.34)	12(t=0.65-1.34)
Changing (1)	6(t=1.34-2.06)	10(t=1.34-2.06)	12(t=1.34-2.06)
	22(others)	10(others)	12(others)
Load	22(t=0.70-1.35)	20(t=0.70-1.35)	12(t=0.70-1.35)
Changing(2)	22(others)	10(others)	12(others)
V_g and load	14.5(t=0.67-1.27)	20(t=0.67-1.27)	6(t=0.67-1.27)
Changing (3)	14.5(others)	10(others)	12(others)
Proposed AMPC with Estimated DNN Controller			
Reference	14.5(t=0.66-1.36)	10(t=0.66-1.36)	12(t=0.66-1.36)
Changing (1)	6(t=1.36-2.06)	10(t=1.36-2.06)	12(t=1.36-2.06)
	22(others)	10(others)	12(others)
Load	22(t=0.47-1.06)	20(t=0.47-1.06)	12(t=0.47-1.06)
Changing (2)	22(others)	10(others)	12(others)
V_g and load	14.5(t=0.59-1.25)	20(t=0.59-1.25)	6(t=0.59-1.25)
Changing (3)	14.5(others)	10(others)	12(others)

choice. It should be mentioned that the constrained optimization is done during the prediction horizon. As the prediction horizon increases, the accuracy of each element of the argument vector of the cost function (4) increases and it uses the prediction model to calculate model output during constrained optimization. According to [11], according to the law of the receding horizon (5), only the first element of the argument vector is used to calculate the control variable in each iteration. Larger prediction and control horizon values result in more information from the online estimated model response. Since the model used in AMPC is updated in each iteration of the control loop, this work leads to the improvement of the controller's performance.

B. Offline DNN Estimation Using Basic Constrained AMPC Data and, DNN Output Tuning Method

One of the main goals of this research is reducing the computational demands of the proposed controller. To this end, a linear DNN model has been developed as an alternative to the predictive controller in the specific range around the reference value, especially during the system's steady-state response. The necessary data was collected following the application of the basic AMPC on the system and the DNN-based AMPC method, as detailed in the three tests presented in Table III. The reference voltage changing test has been done for 2.96 s and load and V_g changing tests have been done for 1.96 s for all methods. This study aims to address the practical and industrial applications of the converter and its control algorithm by taking into account the operational conditions of the converter, including the maximum and minimum input load and voltage values. To ensure the offline estimated DNN model for the AMPC controller achieves high accuracy and functions effectively across various operational ranges, the test scenarios outlined in Table III were carefully chosen to cover the full spectrum of the converter's intended performance. After estimating the neural network model, a mechanism has been introduced for switching between the dynamic neural network model and the constrained predictive control. This switch is initiated when the output voltage reaches within 20% of its reference value. Given the fast dynamics of the converter and the need to minimize fluctuations in the control signal, the dynamic neural network model, which more accurately represents the actual system, has been utilized in this study.

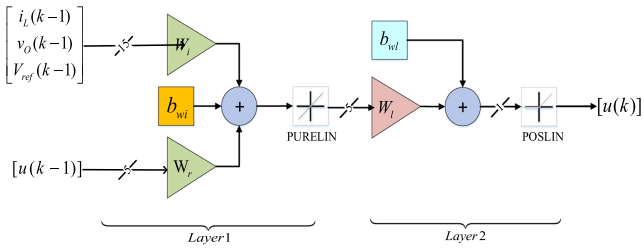

Fig. 2. Block diagram of the estimated DNN model.

For the simplicity of the model, a two-layer dynamic linear neural network (see Fig. 2) with five neurons between both nodes, a total of 25 parameters (hidden layer weights and bias W_i, W_r, b_{wi}), and six parameters (output layer weights and bias W_l, b_{wl}) in the second layer is considered in (6). In the first layer, the activation function is pure linear and in the second layer, it is positive linear. According to the usual routine of neural network estimation [11], 70% of the data was for training, 15% for validation, and 15% for model testing. The model was estimated using the Levenberg–Marquardt (LM) algorithm, with the estimation cost function being the average sum of squared estimation errors. As illustrated in Fig. 3, the model's accuracy for all three data groups was approximately 99%. The model inputs are the converter's input current, its output voltage, and the voltage reference value. The DNN output is the control variable for the duty cycle of the switches

$$u(k+1) = \text{DNN}\left(u(k), v_o(k), i_L(k), V_{ref}, W_i, W_l, W_r, b_{wi}, b_{wl}\right) \tag{6a}$$

$$R = 1 - \frac{\|u_{\text{real}} - u_{\text{estimated}}\|}{\|u_{\text{real}} - u_{\text{mean of real data}}\|}. \tag{6b}$$

The R parameter indicates the fit of the DNN model's output to the real data, which is more than 99% according to Fig. 3(a). Choosing the first-order DNN dynamic model for the equivalent controller, unlike the feed forward ANN where the output at each moment depends on the input at the same moment, results in a smoother model output and reduces the impact of outliers and measurement noise. Additionally, the data used to estimate the DNN from the AMPC controller is collected from the real system using the KRLS one-step-forward algorithm to estimate the system model. Using the KRLS regression algorithm effectively reduces the impact of outlier data and measurement noise, resulting in cleaner data overall.

Fig. 3 shows that the model was correctly estimated using the LM algorithm in only eight epochs. The gradient of the estimation error has converged to a small value and the adaptation parameter μ has reached its maximum value in eight repetitions, which means that the estimation of the model has been as accurate as possible [11], which is the result of the estimation of the model for four categories of training and validation data training and total data confirm that matching

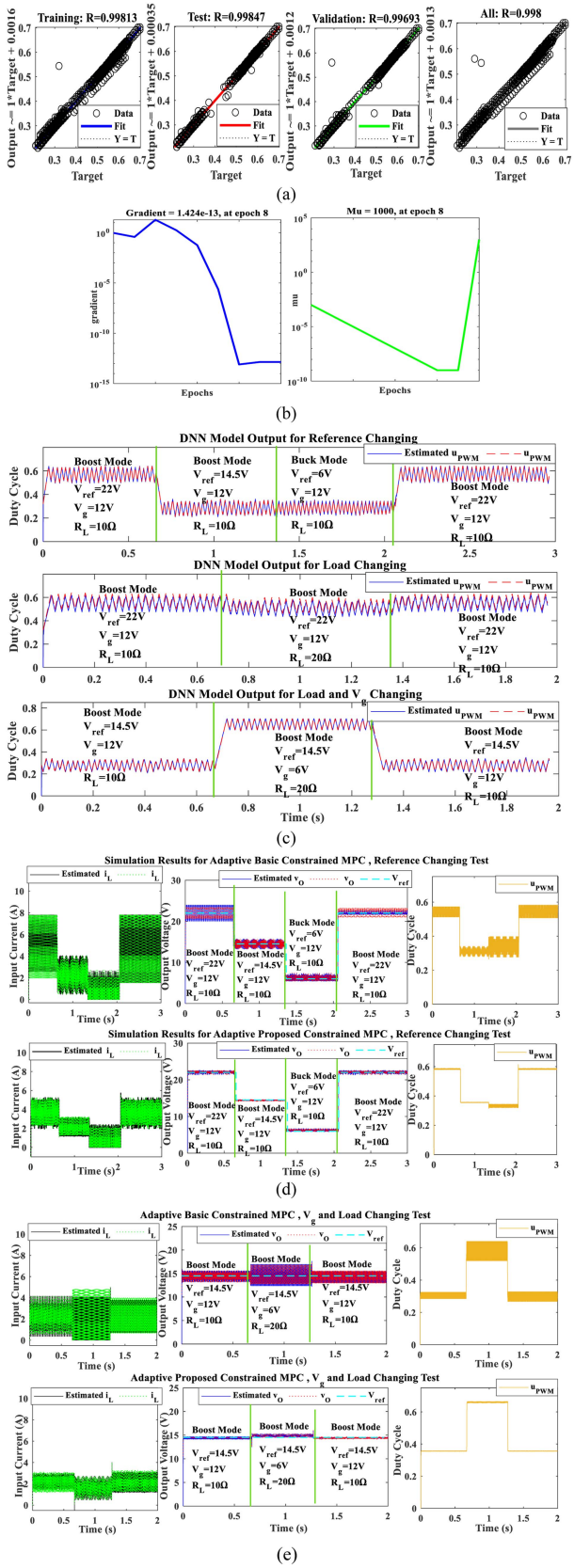

Fig. 3. DNN estimation results using experimental data include (a) fitting degree, (b) estimation gradient, and (c) control variable for adaptive MPC data and estimated DNN. Simulation results for basic and proposed AMPC: (d) reference changing test (e) load and, input voltage test.

rate of model output data with real converter data is about 99%. According to [26], θ_{LM} is a vector of parameters. N_t is the total number of samples and n is the total number of parameters. J_{LM} is the Jacobian matrix of the estimation error, which aims to estimate the minimization of the function $V(\theta_{\mathrm{LM}})$ (the mean square of the estimation error). $\nabla V(\theta_{\mathrm{LM}})$ is the gradient matrix of estimation error and $\nabla^2 V(\theta_{\mathrm{LM}})$ is the Hessian matrix. μ is the learning coefficient of the network, which has an important effect on the convergence of parameters. This coefficient is adjusted according to the interval defined for it during network training. $\Delta(\theta_{\mathrm{LM}})$ is the result of the LM algorithm in each step. Overall equations of the LM algorithm are described as follows (7) the DNN model estimation has been done in MATLAB:

$$V\left(\theta_{\mathrm{LM}}\right)=\frac{\sum_{i=1}^{N_t} e_i^2\left(\theta_{\mathrm{LM}}\right)}{N_t},\ \theta_{\mathrm{LM}}=\mathrm{DNN}\left(W_i, W_r, b_{wi}, W_l, b_{wl}\right)$$

$$e_k\ \left(\theta_{\mathrm{LM}}\right)=u_{\mathrm{real}}(k)-u_{\mathrm{estimated}}(k)$$

$$\nabla V\left(\theta_{\mathrm{LM}}\right)=J_{\mathrm{LM}}^T\ \left(\theta_{\mathrm{LM}}\right) e\left(\theta_{\mathrm{LM}}\right)$$

$$\nabla^2 V\ \left(\theta_{\mathrm{LM}}\right)=J_{\mathrm{LM}}^T\ \left(\theta_{\mathrm{LM}}\right) J_{\mathrm{LM}}\left(\theta_{\mathrm{LM}}\right)+S\left(\theta_{\mathrm{LM}}\right)$$

$$S\left(\theta_{\mathrm{LM}}\right)=\sum_{i=1}^{N_t} e_i\left(\theta_{\mathrm{LM}}\right) \nabla^2 e_i\left(\theta_{\mathrm{LM}}\right) \tag{7a}$$

$$\begin{cases} J_{\mathrm{LM}}\ \left(\theta_{\mathrm{LM}}\right)=\begin{bmatrix} \frac{\partial e_1}{\partial \theta_{\mathrm{LM},1}} & \frac{\partial e_1}{\partial \theta_{\mathrm{LM},2}} & \cdots & \frac{\partial e_1}{\partial \theta_{\mathrm{LM},n}} \\ \frac{\partial e_2}{\partial \theta_{\mathrm{LM},1}} & \frac{\partial e_2}{\partial \theta_{\mathrm{LM},2}} & \cdots & \frac{\partial e_2}{\partial \theta_{\mathrm{LM},n}} \\ \vdots & \vdots & \ddots & \vdots \\ \frac{\partial e_{N_t}}{\partial \theta_{\mathrm{LM},1}} & \frac{\partial e_{N_t}}{\partial \theta_{\mathrm{LM},2}} & \cdots & \frac{\partial e_{N_t}}{\partial \theta_{\mathrm{LM},n}} \end{bmatrix} \rightarrow \text{Jacobian} \\ \Delta\left(\theta_{\mathrm{LM}}\right)=\left[J_{\mathrm{LM}}^T\left(\theta_{\mathrm{LM}}\right) J_{\mathrm{LM}}\left(\theta_{\mathrm{LM}}\right)+\mu I\right]^{-1} J_{\mathrm{LM}}^T\left(\theta_{\mathrm{LM}}\right) e\left(\theta_{\mathrm{LM}}\right) \\ \quad \xrightarrow{S(\theta_{LM})\approx 0} \\ \quad \rightarrow \mathrm{LM}\theta_{\mathrm{LM,New}}=\theta_{\mathrm{LM,Old}}+\Delta\left(\theta_{\mathrm{LM}}\right). \end{cases} \tag{7b}$$

According to the previous section, it is understood that a complex controller like constrained AMPC is effective in managing the buck–boost dc converter. However, when this controller is simplified to just a linear DNN for implementation in a real system, discrepancies may arise compared to the reference value. This is particularly noticeable in steady-state mode due to changes in system conditions. To mitigate this error, a regulation mechanism has been incorporated. This mechanism relies on the output voltage error and employs a constant coefficient to refine the adjustment of the duty cycle control variable in the DNN output. Additionally, the control signal constraint, which is a feature in the constrained AMPC method, is also integrated into this regulation mechanism. Below the equations pertaining to this method are described in (8). k_c and k_{cn} are constant coefficients of the control variable tuning

$$\begin{cases} \text{if } \left((e\ (k)=V_{ref}-v_O\,(k))>0\right) \\ u_{\mathrm{DNN}}\,(k+1)=\min\left(\max\left(u\,(k+1)+k_c e\,(k)\,, u_{\min}\right),\ u_{\max}\right) \\ \qquad else \\ u_{\mathrm{DNN}}\,(k+1)=\min\left(\max\left(u\,(k+1)+k_{cn} e(k), u_{\min}\right), u_{\max}\right). \end{cases} \tag{8}$$

According to (8), and (9), it is evident that the performance of this mechanism depends on adding or subtracting a value from the DNN output control variable to minimize the steady-state error of the system. This is particularly crucial when the system encounters undefined disturbances. To enhance this mechanism's performance, the adjustment factor for the positive and negative time of the output voltage error differs from the reference value. This change increases the mechanism's degree of freedom. The reason is that the adaptive model's estimation part, which uses the Kalman filter and the constrained AMPC controller, relies on the real-time numerical solution of their respective equations, as there is no preformulated package solution available. The selection of coefficients k_c, k_{cn} for the proposed mechanism in this section involves repeated tests and examination of experimental results. These results are within 20% of the output voltage error compared to the reference value, which aligns with the activation range of the DNN-based mechanism mentioned in the previous section. This method aims to minimize the error and fluctuations in the output voltage's steady-state response. If the value of these coefficients increases excessively, the response will become more fluctuating due to the expanded range of the control variable for the output voltage. Conversely, if their value decreases significantly, it may lead to an increased error in the output voltage compared to the reference value. Additionally, the upper and lower limits of the control variable have been implemented in the proposed mechanism, as outlined in Section III-A, using the min-max function

$$\begin{cases} k_c = 0.002 \\ k_{cn} = 0.002. \end{cases} \tag{9}$$

The proposed AMPC method diagram is shown in Fig. 4.

To summarize, the final value of the control variable is determined by choosing between the outputs of the adaptive constrained AMPC controller, detailed in (4) and (5) and illustrated in Fig. 4, and the DNN model presented in (8). Additionally, the method for calculating the pulse-width modulation (PWM) duty cycle of the switches is outlined in

$$\begin{cases} if\ (|v_O - V_{ref}| > 0.2{*}V_{ref}) \rightarrow\ u_{\mathrm{PWM}} = u_{\mathrm{MPC}} \\ if\ (|v_O - V_{ref}| \leq 0.2 * V_{ref}) \rightarrow\ u_{\mathrm{PWM}} = u_{\mathrm{DNN}} \end{cases} \tag{10a}$$

$$\begin{cases} if\ (V_{ref} \leq V_g) \rightarrow\ u_{S1} = u_{S2}\ = u_{\mathrm{PWM}} \\ if\ (V_{ref} > V_g) \rightarrow\ u_{S1} = 1,\ u_{S2} = u_{\mathrm{PWM}} \end{cases} \tag{10b}$$

where u_{PWM} is the main control variable of the two switches; u_{S1} and, u_{S2} are the control variables of each switch. According to Fig. 4, the proposed AMPC method maintains switch *S1* in the closed state in boost mode to effectively reduce switching losses and stabilize input current fluctuations, thereby ensuring quicker convergence of the output voltage to the desired value. The state-space model described in (1) significantly simplifies control computations by allowing both switches to be controlled with a single variable, offering a substantial advantage [17]. Within the AMPC controller, imposing constraints on the control variable enhances the system's stability. The control variable's changes constraint at each step, results softening the output voltage and control variable, which helps reduce inrush current during the converter's transient responses and prevents voltage overshoot.

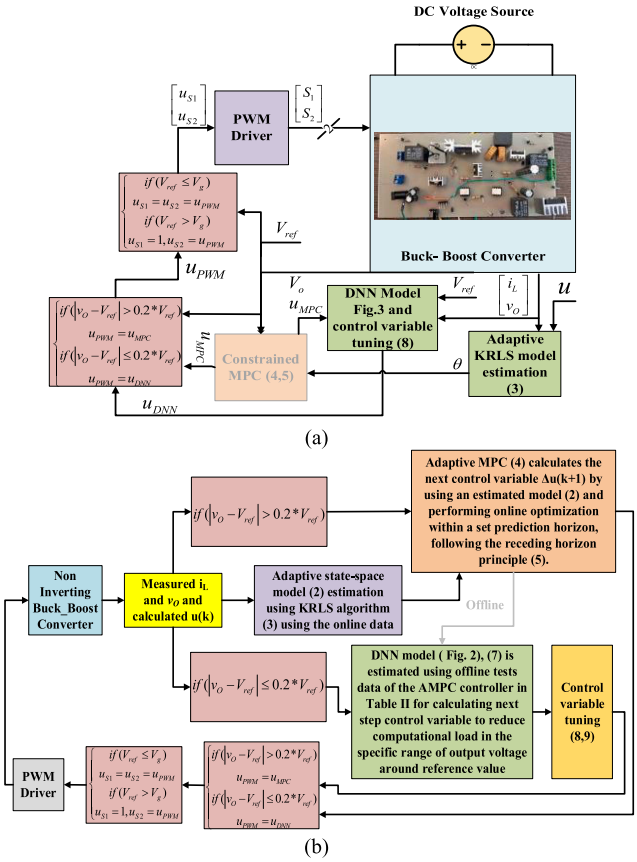

Fig. 4. Proposed AMPC method (a) block diagram and (b) flow diagram.

Two points need to be addressed. First, as noted earlier [24], the adaptive mechanism in controllers is based on the online state-space model (2) estimation using the KRLS algorithm, that results improving system robustness in presence of big dynamic changes and disturbances. Selecting the control variable's changes, Δu_{MPC} as the main optimization argument in the cost function (5) boosts controller performance by smoothing changes in the control variable during disturbances. By adjusting the weight coefficients in (5) offline through repeated tests, as shown in Table III, the controller maintains optimal performance within the considered working range. Second, the selected KRLS algorithm for online model estimation is a fast and recursive method with minimal computational demand. It is deployed alongside the AMPC during the system's transient response to changes in reference, load, or input voltage, ensuring the controller's effectiveness. When the converter's output voltage aligns closely with the reference value and the system stabilizes, control shifts to the DNN model, which adjusts the output based on voltage error. However, the KRLS algorithm remains active, continuously estimating the system's state-space model, ensuring that the model used by the AMPC is always ready to maintain optimal performance, even when the system's operational mode changes.

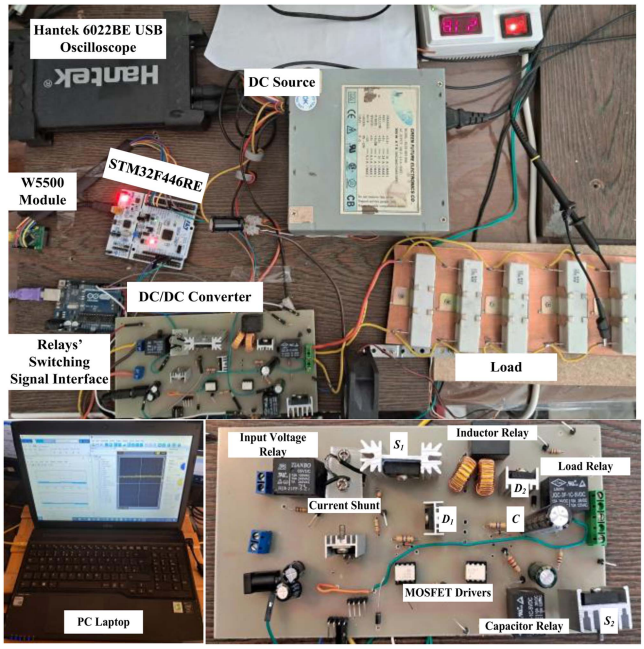

Fig. 5. Overview of experimental setup components.

This study is entirely data driven. It specifically utilizes real system data for both the adaptive mechanism of model estimation in the AMPC controller and the DNN model estimation, including its output adjustment mechanism. Experimental data from the actual system was employed throughout to present the results and conduct all analyses. To further validate the efficacy of the proposed control method, computer simulations were performed using Simulink. Fig. 3 illustrates the outcomes of two tests: changing the reference output voltage and simultaneously altering the load and input voltage for both the standard and proposed AMPC methods using estimated DNN. Fig. 3(d) and (e)'s simulation data for the reference value change test shows that with the basic AMPC method, the output voltage fluctuation reaches 2 V at a 22 V reference, and 1 V at 14.5 and 6 V references. However, with the proposed method, the fluctuation range narrows to 0.5 V–0.6 V for these reference values. In the load and input voltage change test, the standard method exhibited about 1 V of fluctuation at a 10 Ω load and 12 V input, and 1.5 V–2 V at a 20 Ω load and 6V input. Conversely, the proposed method maintained a consistent fluctuation of about 0.5 V.

IV. Experimental Results

The experimental setup consists of two main components: a noninverting buck–boost converter and a control interface, along with the associated hardware, as depicted in Fig. 5.

A. Main Tests

According to Table III, the proposed combinatorial adaptive constrained MPC has been implemented in the system. The experimental outcomes for the three tests are detailed, encompassing changes in reference voltage (test 1), load variations (test 2), and both input voltage and load changes (test 3). It is important to note that in all three tests, the timing of the changes is arbitrary, and the control algorithm is unaware of when these changes occur. In other words, these changes are not modeled in the controller. The aim is to make the conditions of the laboratory setup as similar as possible to the operating conditions of real systems. In real systems, only the variation range of the reference voltage, load, and input voltage is known in their operational chart. Even the input dc voltage source is not ideal.

Test 1 describes about altering the value of the reference voltage to assess the controller's performance in both boost and buck modes. Test 3 presents the most significant challenge, as it involves simultaneous changes in the input voltage and load. Due to the nonlinear relationship of the converter's state variables, maintaining the controller's optimal performance during this test is crucial. These results have been compared with those obtained using the basic adaptive constrained MPC. The comparative findings are presented in Fig. 6.

In the basic AMPC method (for example in [12]), the numerical solution of the optimization algorithm causes fluctuations in the control signal each time the control algorithm is executed. This is due to the cost function's argument having a value, leading to increased fluctuations in both the input current and output voltage of the dc converter. In contrast, the proposed method utilizes an estimated DNN model in place of the controller for the system's steady-state response. Based on its dynamic nature, this approach results in smaller changes and significantly reduced oscillations in the control signal compared to the basic AMPC also it causes smooth transient especially in the changing between boost and buck mode according to Fig. 6. Consequently, the control signal converges to a specific value, and the input current fluctuations of the converter are diminished. Regarding the output voltage, the average fluctuation is approximately 1.3 V (72%) less than that of the basic method across the three described tests and the maximum oscillation domain of the output voltage around the reference value is about 0.5 V. Additionally, the proposed method's model estimation algorithm KRLS [see Figs. 6 and 7(b)], achieves fast model estimation with fewer oscillations. Also, the binding mechanism of control variable adjustment has helped to reduce the steady-state error of the system as much as possible compared to the reference value. In terms of the peak input current of the system, due to the constraint on the control variable and its changes, for the basic AMPC method, this value is about 7.2 to 8 A for the 22 V output, and for the proposed AMPC method, this value is about 6 to 7 A. For the output of 14.5 V, this value is about 4.5 A for the basic method and 3.5 A for the proposed method. Based on Fig. 6(c), it is clear that for both main controllers and during the test of simultaneous changes in input voltage and load, the amplitude of output voltage oscillations in the proposed method is about 1.2 V less than in the baseline method. In the system's transient response at the beginning of the test, due to the output voltage change from 10 V to 14.5 V, the response is quick, and the overshoot in the baseline method is small. To better demonstrate the performance of the proposed controller, this figure is zoomed in. In the system's transient response (reducing overshoot about 1.5 V) during load and input voltage changes, which are distinguished by green lines in the relevant figure,

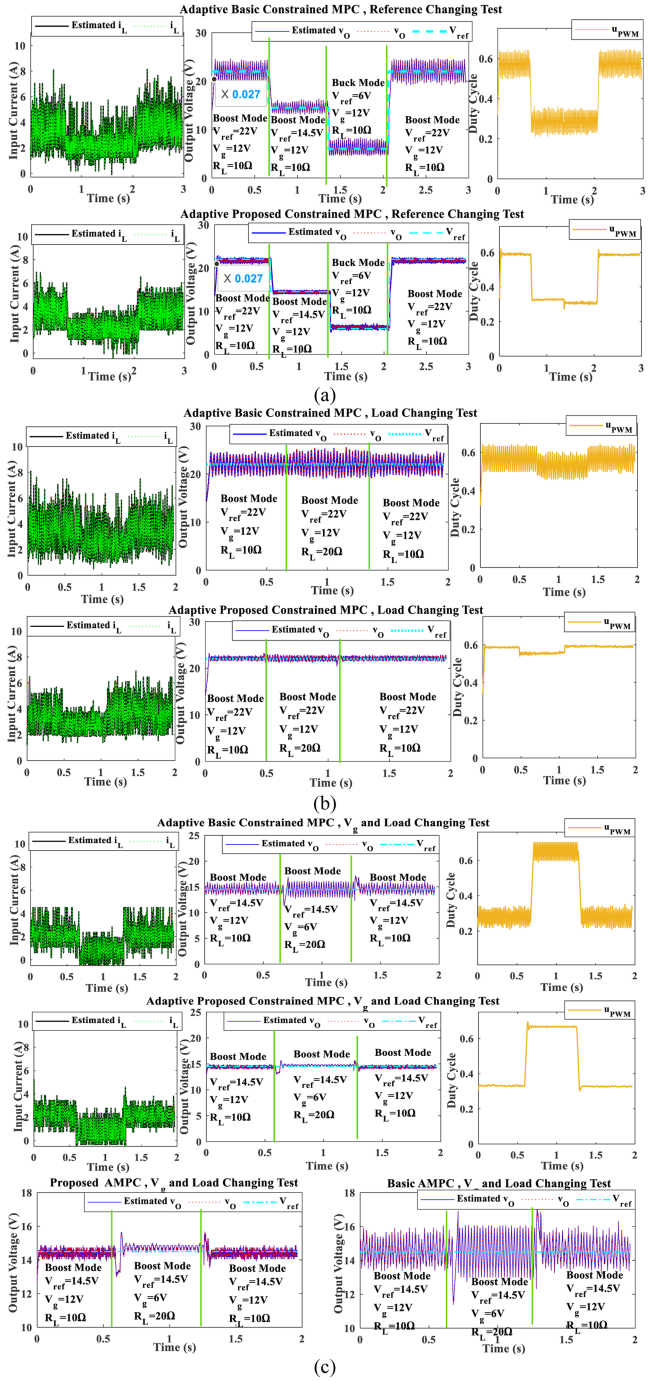

Fig. 6. Basic and proposed combinatorial constrained AMPC methods results: (a) reference voltage changing, (b) load changing, (c) input voltage and load changing tests, and (d) estimated model parameters using the proposed method.

the positive effect of the proposed method on improving the system's response is clearly shown.

Fig. 7(a) illustrates the poles of the discrete state space model for the real closed-loop system, derived in real-time from the state and control variables. It is noted that these poles, as computed by MATLAB for the closed-loop model, are consistently real-valued and located within the unit circle for all three conducted tests. This indicates a maintained stability of the

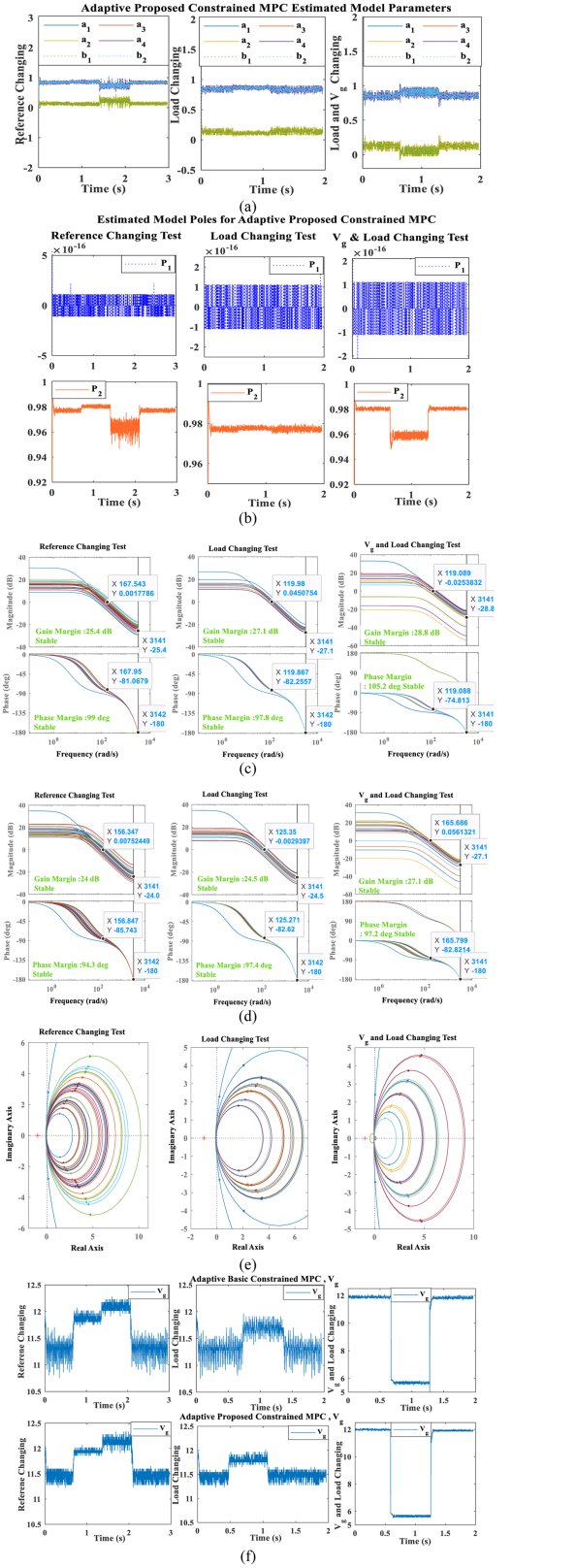

Fig. 7. Proposed combinatorial constrained AMPC method results: (a) estimated discrete state-space system model parameters using the proposed method and (b) estimated discrete state-space model poles using closed-loop data. The bode diagram of the estimated discrete state-space model output every 100 samples using the (c) proposed AMPC. (d) Basic AMPC. (e) Nyquist diagram of the estimated discrete state-space model output for each 100 samples using the proposed AMPC experimental data. (f) Input voltage V_g of nonideal regular power supply.

closed-loop system with respect to [27]. Furthermore, the mechanism proposed emphasizes the system's steady-state response over its dynamic response within a specific range close to the reference value. To minimize computational effort, an offline estimated DNN utilizing AMPC data within this operational range supersedes the existing algorithm. According to [27], it is mentioned that the closed-loop system's poles [see depicted in Fig. 7(a)], indicate an absence of inherent oscillation in response to step inputs. Oscillations in this system's output, when employing model-based controllers, stem solely from input fluctuations, implying they can happen at the steady-state response. In contrast, the traditional AMPC method, which relies on constrained numerical optimization for computing control variable changes at each iteration, inherently experiences fluctuations because of that mechanism. However, substituting it with DNN, a first-order dynamic model, helps in reducing the variation of the control variable, thus stabilizing output voltage fluctuations to a consistent value. The DNN output adjustment mechanism based on the output voltage error from the reference value also helps to reduce the steady-state error.

Fig. 7(c) and (d) presents the Bode plot for the estimated parameters of the system's discrete state-space model. These plots, sampled every 100 data points at the highest frequency range according to the Nyquist criterion π/Ts, demonstrate stability in both gain and phase within the designated frequency range [27]. Both the basic and proposed AMPC methods ensure positive phase and gain margins in the Bode diagrams, indicating the stability of the discrete model within the specified frequency range. The proposed method shows slightly higher phase and gain margins. Furthermore, the consistent response of the Bode diagrams in the proposed method across different time samples of the estimated state-space model suggests less variability in the estimated model parameters across the three tests, indicating a more uniform frequency response of the closed-loop system. This consistency highlights the superior performance of the adaptive mechanism in the proposed AMPC method. These figures also identifies optimal points for calculating the phase and gain margins. Fig. 7(e) presents the Nyquist diagram for the discrete model of the closed-loop system. According to the Nyquist stability criterion, for a closed-loop system to be stable, the Nyquist plot must not encircle the point (-1+j0). Additionally, the number of clockwise encirclements of the point (-1+j0) by the Nyquist plot must equal the number of poles of the open-loop transfer function that are outside the unit circle in the z-plane. The Nyquist diagrams, combined with Fig. 7(a) showing that the poles of the discrete model are inside the unit circle for all three tests, confirm that Nyquist stability has been established in this research.

Fig. 7(f) shows the output voltage from the nonideal dc power supply in the experimental setup, which deviated from ideal conditions. In the three loaded tests, the maximum voltage fluctuated between 11 V and 12.5 V. Despite this, the controllers managed to stabilize the output voltage effectively. The proposed AMPC method has reduced the input voltage fluctuations during the operation of the dc converter, thereby increasing the lifetime of the dc power supply between 11 V and, 12.5 V. Despite this, the controllers managed to stabilize the output voltage effectively. The proposed AMPC method has reduced the input voltage fluctuations during the operation of the dc converter, thereby increasing the lifetime of the dc power supply. One essential requirement for bounded MPC methods, especially in power electronic converters, is that the control board's processor must have sufficient processing power. This is crucial to complete the control loop quickly, given the system's rapid dynamics. As technology has advanced, processors have become more powerful and compact. However, their thermal power generation has increased, leading to gradual CPU deterioration over time. This study notes that since a converter predominantly operates in its steady state, using a linear neural network model for the AMPC control in this mode significantly reduces the computational load. To enhance the practicality of the research, an affordable STM32 board with an F4 processor operating up to 180 MHz and costing about $16 has been used. This board, ideal for interfacing with PC computers through a compatible module, leverages an ARM microcontroller. By using MATLAB's code generation toolbox, control algorithm codes were efficiently translated from MATLAB to C language and uploaded to the board. For future advancements, upgrading to more sophisticated boards with F7 or H7 processors, which offer higher CPU frequencies, might boost control method performance. This reduction is primarily observed during the system's transient response, where implementing the constrained AMPC control algorithm is crucial. Lowering the computational load also decreases the energy consumption of the control hardware. From the perspective of reducing the computational burden, the proposed method generates about 93.7% of the total 6892 needed control variable (duty cycle) values using the DNN model, with only 6.3% generated by the constrained AMPC mechanism in three reference, load, and input voltage changing tests. Adaptive online model estimation is effectively implemented in both controllers. The total sampling time (T_s) in this research includes three parts: 1) measuring the input current and output voltage of the converter, 2) executing the control algorithm, and 3) generating PWM signals. To compare the four controllers implemented on the converter, the total sampling time for all methods is 1 ms. The average time required to run the AMPC algorithm based on the experimental setup is 438 μs. The time required to execute the proposed AMPC method is 106 μs, about 75% less than the traditional AMPC method.

In the following analysis, the performance of the proposed controller is compared with that of a PI controller. PI controllers are widely used to control many dc converters due to their simple implementation and minimal computational demand. In this study, the PI controller is designed based on the Bode and Nyquist diagram of the closed-loop system for the proposed AMPC, as shown in Fig. 7(c) and (f), and, using [27], [28]. In [28] the developed method approximates the derivatives of amplitude and phase responses of a plant model by Bode's integrals, eliminating the need for an actual plant model. This approach helps adjust the slope of the Nyquist diagram to enhance closed-loop performance. Additionally, these derivatives aid in calculating the gradient and Hessian for a frequency criterion in iterative PID tuning. The frequency criterion is the total squared difference between the targeted and actual gain margin, phase margin,

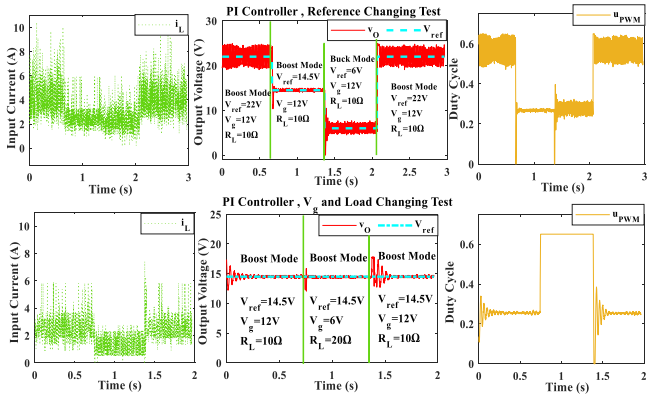

Fig. 8. Reference, input voltage, and load-changing tests results for the PI controller.

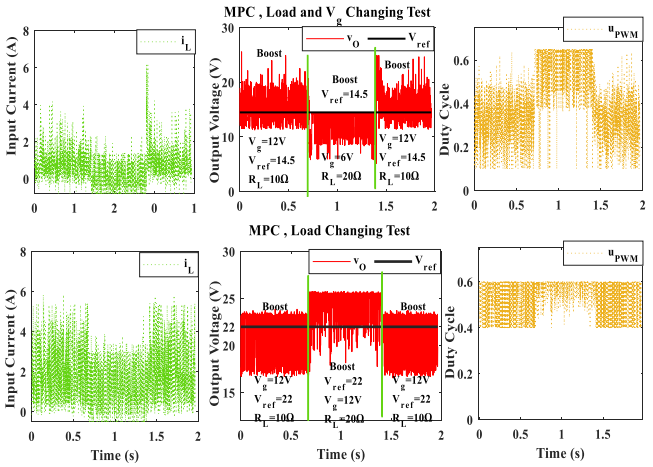

Fig. 9. Input voltage and load changing tests results for the developed MPC in [17].

and crossover frequency. This method utilizes the advantages of closed-loop system characteristics such as gain margin, phase margin, and crossover frequency. Because the converter has fast and nonlinear dynamics, in order to reduce the fluctuations of the output voltage and the control variable, the derivative coefficient of the controller is set equal to zero and the controller is applied in the form of PI on the converter. According to what was described, by repeating the tests and checking it for the real system, the coefficients of the proportional and integral parts of the PI controller are equal to $k_P = 0.02$ and, $k_I = 0.0075$, respectively.

However, the PI method has several disadvantages, including the limited capability to consider constraints on the control variable and adapt to changes during the computation of the control signal. It also offers a low degree of freedom and presents a challenge in adjusting the controller parameters to achieve optimal performance. This is while ensuring the convergence speed of the output to the reference value remains efficient across different modes, which is particularly challenging for nonlinear systems. Also, the presence of constraints on the control variable and its changes in the target AMPC controller helps the stability of the closed loop system.

Fig. 8 indicates that with a reference value of 22 V, the fluctuation range is approximately 2.5 V. When the reference is changed to 14.5 V, the undershoot is about 4 V, and the fluctuation range is around 1.3 V. Entering buck mode with a reference voltage of 6 V results in both overshoot and undershoot within a 4-V range, accompanied by fluctuations of about 3 V. During the load change test, with an input voltage of 14.5 V, the overshoot for the reference is 2.5 V, and the fluctuation range is approximately 1.3 V. For the PI method, due to the absence of restrictions on the control variable and its changes, the peak input current for the output voltage of 22 V is about 9 to 10 A, and for the output voltage of 14.5 V, this value is about 6 A.

In order to clarify the performance superiority of the proposed combinational AMPC controller, the results of two challenging tests 1 and 2 have been applied to the controller proposed in research [17], and their results are shown in Fig. 9. Parameters of this controller are also selected according to [17]. According to Fig. 8 and [17], following points can be stated.

1) In the relevant control method, the calculation of controller coefficients depends on the precise model of the system. When the setup and working conditions of the system change, the results differ even if the converter parameters remain the same. However, in the proposed method, model estimation is performed online.
2) Constraints on the control variable are limited to its upper and lower limits, while its changes are unrestricted. This has led to fluctuations within a relatively large range at certain times in the control variable. Moreover, calculations during the prediction horizon are confined to forecasting just the next step, providing limited insight into the system's future behavior under the desired working conditions.
3) For optimal controller performance, accurately calculating not only the reference value of the output voltage but also the reference values for the input current and the control variable is necessary.
4) The results from related research indicate that in boost mode, the output voltage of the converter fluctuates within a range of 4 V–5.5 V when the input voltage is increased by 1.5 to 2 times. As depicted in Fig. 9, during test 2 (which involved a change of load) with an input voltage of 12 V a reference voltage of 22 V under normal conditions, and a 10 Ω load, the output voltage's maximum fluctuation was approximately 4 V, which is less than the reference value. Upon increasing the load to 20 Ω, the output voltage exhibited an overshoot of approximately 5.5 V compared to the reference value. In test 3, where there was a simultaneous change in load and input voltage, with an input voltage of 12 V and a reference voltage of 14.5 V, the maximum overshoot in output voltage was 5.5 V. After altering the input voltage to 6 V and the load to 20 Ω, the maximum undershoot value in the output voltage is 4.5 V. These fluctuations primarily stem from the controller's dependence on an accurate system model, a limited prediction horizon, and challenges in selecting

TABLE IV
EXPERIMENTAL RESULTS OBTAINED BY DIFFERENT METHODS, TS = 1 MS

Test	S_1, S_2 Resistive Energy Losses (J)	L Resistive Energy Losses (J)	Sum of Squares Error of v_o (V)	v_o (V) Maximum Oscillation Domain	i_L (A) Maximum Oscillation Domain	Mean of Computational Time (μs)
			Basic AMPC			
Ref Changing	2.49,0.68	1.46	7591.9	1.8	8	438
Load Changing	2.09,0.57	1.23	4503.4	1.8	8	
V_g and load Changing	0.71,0.19	0.42	1253.9	2	4.7	
			DNN-based Proposed AMPC			
Ref Changing	2.33,0.56	1.37	4261.3	0.5	7	106
Load Changing	1.97,0.50	1.16	1033.3	0.5	6.2	
V_g and load Changing	0.64,0.15	0.37	228.34	0.5	3.84	
			PI Controller			
Ref Changing	3.26,1.04	1.92	7437.1	2.5-3	10	69
V_g and load Changing	0.96,0.28	0.56	594.33	1.3	7	
			Ref [17]			
Load Changing	2.07,0.59	1.83	16641	4	5.9	84
V_g and load Changing	0.73,0.17	0.49	18010	5.5	6	

the correct reference values for output voltage, control variable, and input current.

In this research, the primary goal is to examine the impact of control methods on the converter's performance. Consequently, the energy consumption analysis has been conducted in a general manner.

To elucidate the effects of the control methods on the converter's performance, the efficiency [29] ($\eta_{\text{Energy}} = \frac{E_{\text{out}}}{E_{\text{in}}}$) was determined by calculating the ratio of output energy E_{out} to input energy E_{in} for the basic, proposed AMPC methods, and the PI controller, as illustrated in Fig. 10(a). This efficiency is based on the total input and output energy for each of the three tests.

Fig. 10(a) shows that the total performance efficiency of the converter for the proposed AMPC method is 2.5% to 3% higher than the basic method and about 10% to 15% higher than the PI method. Fig. 10(b) shows that for the constrained AMPC method, the target of the average dissipated resistive energy of the switches is about 8.5 to 10% less than the basic method. Also, the average energy dissipation of the inductor for the proposed method is about 8.3% less than the basic method. According to [29], a minimum efficiency of 80% for a noninverting buck–boost converter is generally acceptable, especially in applications where the design prioritizes cost-effectiveness and simplicity over maximum efficiency. The efficiency for AMPC controller is more than 93.5%. Additionally, Fig. 10(b) illustrates the impact of reduction in output voltage fluctuations and input current after implementing the proposed AMPC method compared to the basic method on the resistive energy dissipation in switches S_1 and S_2 ($R_{DS} = 0.085\ \Omega$) and, the inductor L ($r_{\text{Inductor}} = 0.05\ \Omega$). Also, Table IV demonstrates that, for the proposed method across the three tests conducted, the switches' resistive energy losses are lower than those specified with the other three controllers. The discrepancy in output voltage relative to the reference value (encompassing both transient and steady-state responses) is also lower. Additionally, the maximum amplitude of output voltage fluctuations is reduced compared to the other three controllers. This improvement is evident from an overall control point of view [17]. However, in the output power range of 10.5 W to 48 W, the performance efficiency of the converter using the proposed AMPC method is approximately 2% to 3% higher than the basic AMPC.

This research focuses on enhancing the performance of model-based controllers and increasing their flexibility for use in systems of varying complexities, rather than improving the converter structure itself. The results of two basic and proposed AMPC controllers are presented and compared with [17]. These results have been analyzed for a general comparison with the conventional PI controller. As previously mentioned, the drawbacks of the PI controller include limited degrees of freedom, difficulties in optimally tuning the coefficients, and stability issues, particularly in complex systems. During sudden system changes, energy losses increase due to fluctuations in the control variable. Furthermore, the controller is not effective at imposing constraints on control signal changes. Table IV compares the computational load by providing the average time required for each control algorithm. To ensure a fair comparison of all four methods, the overall sampling time for each was set to 1 ms by optimizing the NUCLEO board program. It can be concluded that the proposed method performs adaptively better than other approaches with this sampling time, without the need for continuous controller tuning. This adaptability makes the DNN-based AMPC method suitable for more complex, networked converters with higher computational demands, while also being implementable on less complex systems using cheaper boards. Additionally, this research takes into account both economic and practical considerations. For instance, in the described converter, increasing the capacity of the output capacitor can reduce output fluctuations for a fixed control variable. However, this approach increases the size and cost of the converter, especially at higher power levels. One of the main goals of this research is to reduce the size of converter components to a reasonable level while improving converter performance and stability through enhancements in the proposed AMPC algorithm.

According to Table IV, an important point is that the average calculation time for the traditional AMPC method is around 438 μs, which has been reduced to 106 μs for the proposed

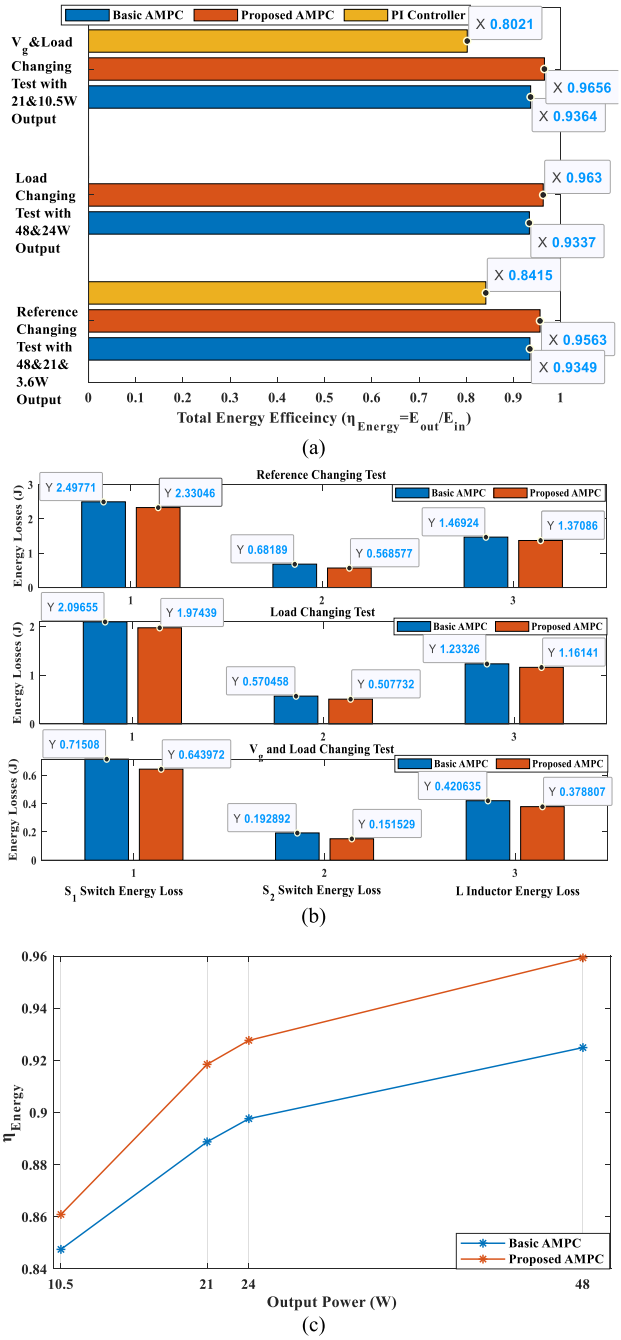

Fig. 10. Reference, input voltage, and load changing tests results for the basic and, proposed AMPC and, PI controller: (a) total energy efficiency, (b) resistive energy losses, and (c) efficiency diagram according to output power for basic and proposed AMPC.

method, representing a significant reduction. In contrast, the PI methods and the MPC method without iterative constrained optimization, and without adaptive model estimation mechanism in [17] involve much simpler calculations, with average calculation times of 67 μs and 84 μs, respectively, for the tests performed. The proposed AMPC method based on DNN model leverages the desirable features of iterative constrained optimization for the system's transient response and its ability to control the

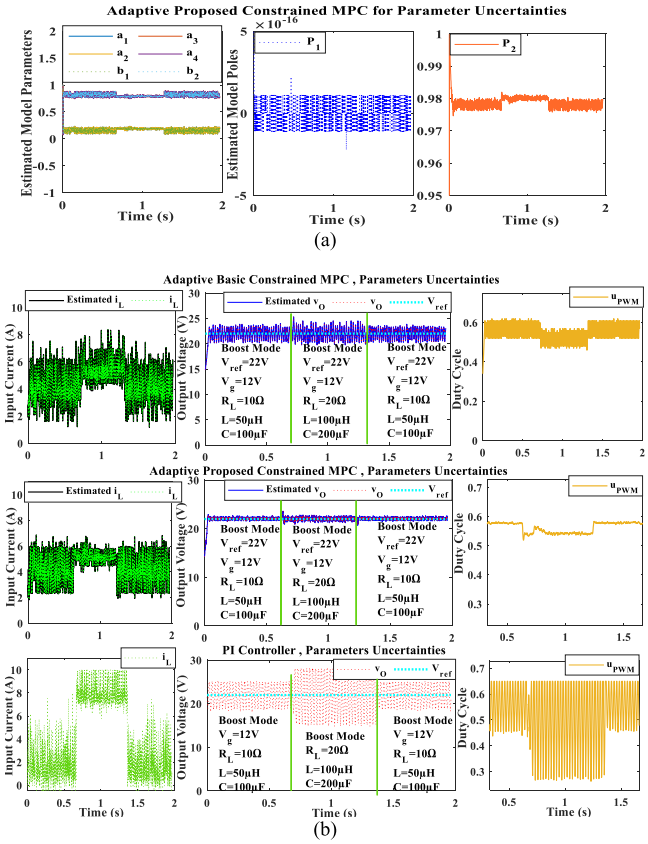

Fig. 11. Basic and proposed combinatorial constrained AMPC, and PI controller methods result for load, capacitor, and inductor changing: (a) estimated closed-loop system model parameters and its poles; (b) output voltage, input current, and control variable.

system in critical situations. The calculation time is acceptable, especially considering that the fluctuations in input current and output voltage are lower than those specified with other methods.

B. Uncertainties Test

In the preceding section, an online load change test was conducted to assess the robustness of the standard and proposed AMPC methods under sudden dynamic changes in the system. Given the dynamic characteristics of the nonlinear converter described in (1), the significance of this test is amplified. This section aims to validate the proposed AMPC method's effectiveness in the presence of uncertainties in the capacities of all passive converter components, such as the output capacitor and inductor, over time. Thus, ensuring the method's robustness and optimal performance to maintain system stability is crucial. In this section, the test recorded a load shift from 10 Ω to 20 Ω, during which the output capacitor's capacity also shifted from 50 μF to 100 μF, using capacitors from two different manufacturers. Additionally, the inductance varied from 50 μH to 100 μH. Fig. 11 displays the experimental results from this test.

Fig. 11(a) illustrates that the proposed method, especially after incorporating parameter uncertainty, maintains minimal

fluctuations in model parameters around a steady value. Additionally, the model's poles, estimated from the closed-loop system, remain within the unit circle, ensuring the system's stability. Enhancing the inductor and capacitor capacity in the dc converter inherently slows down its dynamics. Fig. 11(b) demonstrates that with the proposed AMPC method, despite significant changes to the converter parameters, the output voltage fluctuations remain within a range of 0.5 V to 0.6 V. In contrast, the basic AMPC method shows voltage oscillations at 2.6 V, and the PI method sees oscillations climb up to 5.8 V. Moreover, input current and control variable fluctuations are lower with the proposed method compared to the other two methods.

V. Conclusion

The article introduces an adaptive approach called adaptive constrained MPC to manage the voltage of a noninverting dc buck–boost converter with a maximum output of 48 W. The aim is to limit the control signal and its variations to reduce oscillations in the input current and output voltage. The AMPC utilizes a dynamically estimated linear model via the KRLS algorithm. To enhance the computational efficiency, the DNN leverages data from the AMPC controller within the specified range of the output voltage's steady-state response. Experimental tests were conducted to assess variations in reference voltage, load, and input voltage. Notably, the average fluctuation in output voltage across the three tests is approximately 1.3 V (72%) lower compared to the basic method the maximum oscillation domain of the output voltage around the reference value is about 0.5 V. The proposed method significantly reduces the computational burden by primarily relying on the DNN model, which generates about 93.7% of the total 6892 control signals, with the remaining 6.3% generated by the basic constrained MPC control. More specifically, for the proposed method, the output voltage fluctuation is about 72%, the calculation time is about 75%, and the average energy loss of the switch is 8.5–10% less than the basic AMPC. In the final part of the research, in order to evaluate as much as possible, the resistance of the proposed method against system dynamic changes, the test results of simultaneous change of load, change of capacitor capacity and change of inductor inductance for three basic and proposed AMPC controllers and the PI method are specified. For the proposed method, the fluctuations of the control variable and the output voltage of the converter are less acceptable than the other two methods.

References

[1] D. Yoon, Y. Cho, S. Bae, and J. Lee, "An input-series output-series non-inverting buck-boost converter for 1500V DC bus with wide input and output voltage ranges," *IEEE Trans. Ind. Electron.*, vol. 70, no. 11, pp. 11231–11241, Nov. 2023.

[2] J. Moon et al., "60-V non-inverting four-mode buck–boost converter with bootstrap sharing for non-switching power transistors," *IEEE Access*, vol. 8, pp. 208221–208231, 2020.

[3] M. Kabalo, D. Paire, B. Blunier, D. Bouquain, M. G. Simões, and A. Miraoui, "Experimental validation of high-voltage-ratio low-input-current-ripple converters for hybrid fuel cell supercapacitor systems," *IEEE Trans. Veh. Technol.*, vol. 61, no. 8, pp. 3430–3440, Oct. 2012.

[4] Y. Zhang, X.-F. Cheng, and C. Yin, "A soft-switching non-inverting buck–boost converter with efficiency and performance improvement," *IEEE Trans. Power Electron.*, vol. 34, no. 12, pp. 11526–11530, Dec. 2019.

[5] B. Long et al., "Power losses reduction of T-type grid-connected converters based on tolerant sequential model predictive control," *IEEE Trans. Power Electron.*, vol. 37, no. 8, pp. 9089–9103, Aug. 2022.

[6] L. Xu, R. Ma, R. Xie, S. Zhuo, Y. Huangfu, and F. Gao, "Offset-free model predictive control of fuel cell DC–DC boost converter with low-complexity and high-robustness," *IEEE Trans. Ind. Electron.*, vol. 70, no. 6, pp. 5784–5796, Jun. 2023.

[7] T. Dragičević, "Model predictive control of power converters for robust and fast operation of AC microgrids," *IEEE Trans. Power Electron.*, vol. 33, no. 7, pp. 6304–6317, Jul. 2018.

[8] O. Asvadi-Kermani, B. Felegari, D. Amani, H. Momeni, A. Hajizadeh, and A. Oshnoei, "Adaptive generalized predictive voltage control of a boost converter for peak current reduction in the presence of uncertainties," *IEEE Trans. Ind. Inform.*, vol. 20, no. 8, pp. 10334–10343, Aug. 2024.

[9] T. Dragičević and M. Novak, "Weighting factor design in model predictive control of power electronic converters: An artificial neural network approach," *IEEE Trans. Ind. Electron.*, vol. 66, no. 11, pp. 8870–8880, Nov. 2019.

[10] S. A. Davari, V. Nekoukar, C. Garcia, and J. Rodriguez, "Online weighting factor optimization by simplified simulated annealing for finite set predictive control," *IEEE Trans. Ind. Inform.*, vol. 17, no. 1, pp. 31–40, Jan. 2021.

[11] O. Asvadi-Kermani, B. Felegari, H. Momeni, S. A. Davari, and J. Rodriguez, "Dynamic neural-based model predictive voltage controller for an interleaved boost converter with adaptive constraint tuning," *IEEE Trans. Ind. Electron.*, vol. 70, no. 12, pp. 12739–12751, Dec. 2023.

[12] S. M. Ghamari, F. Khavari, H. Molaee, and P. Wheeler, "Generalised model predictive controller design for A DC–DC non-inverting buck–boost converter optimised with a novel identification technique," *IET Power Electron.*, vol. 15, no. 13, pp. 1350–1364, 2022.

[13] B. Ullah, H. Ullah, and S. Khalid, "Direct model predictive control of noninverting buck-boost DC-DC converter," *CES Trans. Elect. Machines Syst.*, vol. 6, no. 3, pp. 332–339, 2022.

[14] Y. Xiang, H. S.-H. Chung, R. Shen, and A. W.-L. Lo, "An ANN-based output-error-driven incremental model predictive control for buck converter against parameter variations," *IEEE J. Emerg. Sel. Topics Power Electron.*, vol. 12, no. 2, pp. 1230–1248, Apr. 2024.

[15] H. Sartipizadeh, F. Harirchi, M. Babakmehr, and P. Dehghanian, "Robust model predictive control of DC-DC floating interleaved boost converter with multiple uncertainties," *IEEE Trans. Energy Convers.*, vol. 36, no. 2, pp. 1403–1412, Jun. 2021.

[16] H. Sartipizadeh and T. L. Vincent, "A new robust MPC using an approximate convex hull," *Automatica*, vol. 92, pp. 115–122, 2018.

[17] A. Garcés-Ruiz, S. Riffo, C. González-Castaño, and C. Restrepo, "Model predictive control with stability guarantee for second-order DC/DC converters," *IEEE Trans. Ind. Electron.*, vol. 71, no. 5, pp. 5157–5165, May 2024.

[18] X. Li, Y. Liu, and Y. Xue, "Four-switch buck–boost converter based on model predictive control with smooth mode transition capability," *IEEE Trans. Ind. Electron.*, vol. 68, no. 10, pp. 9058–9069, Oct. 2021.

[19] Y. Xiang, H. S.-H. Chung, and H. Lin, "Light implementation scheme of ANN-based explicit model-predictive control for DC–DC power converters," *IEEE Trans. Ind. Inform.*, vol. 20, no. 3, pp. 4065–4078, Mar. 2024.

[20] K. Bi et al., "A model predictive controlled bidirectional four quadrant flying capacitor DC/DC converter applied in energy storage system," *IEEE Trans. Power Electron.*, vol. 37, no. 7, pp. 7705–7717, Jul. 2022.

[21] C. Restrepo, B. Barrueto, D. Murillo-Yarce, J. Muñoz, E. Vidal-Idiarte, and R. Giral, "Improved model predictive current control of the versatile buck-boost converter for a photovoltaic application," *IEEE Trans. Energy Convers.*, vol. 37, no. 3, pp. 1505–1519, Sep. 2022.

[22] X. Weng et al., "Comprehensive comparison and analysis of non-inverting buck boost and conventional buck boost converters," *J. Eng.*, vol. 2019, no. 16, pp. 3030–3034, 2019.

[23] E. F. Camacho and C. B. Alba, *Model Predictive Control*. Springer London (Springer-Verlag London): Springer science & business media, 2013.

[24] K. J. Åström and B. Wittenmark, *Adaptive Control*. Dover Publications, INC, Mineola New York: Courier Corporation, 2013.

[25] O. Asvadi-Kermani, B. Felegari, and H. Momeni, "Adaptive constrained generalized predictive controller for the PMSM speed servo system to reduce the effect of different load torques," *e-Prime-Adv. Elect. Eng., Electron. Energy*, vol. 2, 2022, Art. no. 100032.

[26] M. T. Hagan and M. B. Menhaj, "Training feedforward networks with the Marquardt algorithm," *IEEE Trans. Neural Netw.*, vol. 5, no. 6, pp. 989–993, Nov. 1994.
[27] K. Ogata, *Discrete-Time Control Systems*. Englewood Cliffs, NJ, USA: Prentice-Hall, 1995.
[28] A. Karimi, D. Garcia, and R. Longchamp, "PID controller tuning using Bode's integrals," *IEEE Trans. Control Syst. Technol.*, vol. 11, no. 6, pp. 812–821, Nov. 2003.
[29] H. Fan, "Design tips for an efficient non-inverting buck-boost converter," *Analog Appl. J., Texas Instrum.*, pp. 20–25, 2014. [Online]. Available: https://www.ti.com/lit/pdf/slyt584

Omid Asvadi-Kermani (Graduate Student Member, IEEE) received the B.Sc. degree in control engineering from the University of Tabriz, Tabriz, Iran, in 2018 and the M.Sc. degree in control systems engineering from Tarbiat Modares University, Tehran, Iran, in 2021.

His research interests include artificial intelligence-based adaptive and predictive control in power electronics include dc–dc converters, power converters, and electrical drives.

Arman Oshnoei (Senior Member, IEEE) received the Ph.D. degree in electrical engineering from Shahid Beheshti University, Tehran, Iran, in 2021.

From 2020 to 2021, he was a Visiting Ph.D. Scholar with the Department of Energy (AAU Energy), Aalborg University, Aalborg, Denmark. From 2021 to 2022, he was a Research Assistant with Aalborg University. From 2022 to 2023, he was a Postdoctoral Research Fellow with Aalborg University, where he is currently an Assistant Professor with AAU Energy. His research interests include the control and stability of power electronic-based power systems, energy storage systems for grid and e-mobility applications, battery management systems, and intelligent control strategies.

Dr. Oshnoei was the recipient of the Outstanding Researcher Award by Shahid Beheshti University in 2022. He is currently an Associate Editor with the Smart Grids and Sustainable Energy and Circuit World journals and is the Vice Leader of the Center for Research on Smart Batteries research group at AAU Energy.

Frede Blaabjerg (Fellow, IEEE) received the Ph.D. degree in electrical engineering from Aalborg University, Aalborg, Denmark, in 1995.

From 1987 to 1988, he was with ABB-Scandia, Randers, Denmark. He was an Assistant Professor in 1992, an Associate Professor in 1996, and a Full Professor of power electronics and drives in 1998. In 2017, he was a Villum Investigator. He is an honoris causa with Politehnica University Timisoara, Timisoara, and Romania and Tallinn University of Technology, Tallinn, Estonia. He has authored/coauthored more than 600 journal papers in the fields of power electronics and its applications. He is the coauthor of four monographs and editor of ten books in power electronics and its applications. His current research interests include power electronics and its applications, such as in wind turbines, PV systems, reliability, harmonics, and adjustable speed drives.

Dr. Blaabjerg was the recipient of 33 IEEE Prize Paper Awards, the IEEE Power Electronics Society (IEEE PELS) Distinguished Service Award in 2009, the EPE-PEMC Council Award in 2010, the IEEE William E. Newell Power Electronics Award 2014, the Villum Kann Rasmussen Research Award 2014, the Global Energy Prize in 2019, and the 2020 IEEE Edison Medal. From 2006 to 2012, he was the Editor-in-Chief for the IEEE TRANSACTIONS ON POWER ELECTRONICS. He was a Distinguished Lecturer for the IEEE PELS from 2005 to 2007 and for the IEEE Industry Applications Society from 2010 to 2011 as well as from 2017 to 2018. From 2019 to 2020, he was the President of IEEE PELS. He has been the Vice-President of the Danish Academy of Technical Sciences. He was nominated in 2014–2020 by Thomson Reuters to be between the most 250 cited researchers in engineering in the world.